Superconductivity of MgB_2: Covalent Bonds Driven Metallic

J. M. An and W. E. Pickett
Department of Physics, University of California, Davis, California 95616
(Received 23 February 2001)

A series of calculations on MgB_2 and related isoelectronic systems indicates that the layer of Mg^{2+} ions lowers the nonbonding B π (p_z) bands relative to the bonding σ (sp_xp_y) bands compared to graphite, causing $\sigma \rightarrow \pi$ charge transfer and σ band doping of 0.13 holes/cell. Because of their two dimensionality the σ bands contribute strongly to the Fermi level density of states. Calculated deformation potentials of Γ point phonons identify the B bond stretching modes as dominating the electron-phonon coupling. Superconductivity driven by σ band holes is consistent with the report of destruction of superconductivity by doping with Al.

DOI: 10.1103/PhysRevLett.86.4366 PACS numbers: 74.25.Jb, 74.25.Kc, 74.70.Ad

The dependence of the superconducting critical temperature T_c on structure is unclear after decades of study, and recent discoveries have further confused the issues. In conventional superconductors (the high T_c cuprates compose a special case) it has been generally thought that high symmetry, preferably cubic, is favorable for higher T_c. This trend has held up in elemental superconductors (Nb, La under pressure, at 9 and 13 K, respectively), for binaries [Nb_3(Al, Ge), 23 K [1]], (pseudo)ternaries such as (Ba, K)BiO_3 [2], and even fullerene superconductors (T_c to 40 K [3]).

Recently several intriguing counterexamples to this trend have come to light. Semiconducting HfNCl (and ZrNCl) is a van der Waals bonded set of covalent/ionic bonded layers, but superconducts up to 25 K when doped (intercalated) with alkali metals [4]. There is evidence that the surface layer of solid C_{60} becomes superconducting up to 52 K when it is injected to high hole concentrations [5]. And most recently, it is reported that the layered metal/metalloid compound MgB_2 superconducts at ~40 K [6,7], which is by far the highest T_c for a binary system. The B isotope shift of T_c reported by Bud'ko *et al.* [7] and most other early experimental data [8] suggest conventional BCS strong-coupling *s*-wave electron-phonon (EP) pairing. These examples suggest there are important aspects of two dimensionality (2D) for conventional superconductors that are yet to be understood.

A close analogy for MgB_2, structurally, electronically, and regarding superconductivity, is graphite. Graphite has the same C layer structure as B has in MgB_2. The layer stacking that occurs in graphite is central to its semimetallic character but is not important in our analogy. Graphite is isoelectronic with MgB_2; previous studies have established that the Mg atom is effectively ionized. Finally, graphite becomes superconducting up to 5 K, but only when doped (intercalated) [9]. Both graphite and MgB_2 have planar sp^2 bonding, and in graphite it is well established that three of carbon's four valence electrons are tied up in strong σ bonds lying in the graphite plane, and the other electron lies in nonbonding (p_z) π states. Electron doping of graphite, achieved by intercalating alkali atoms between the layers (Na is the most straightforward case) leads to occupation of otherwise unfilled π states and leads to T_c as high as 5 K. MgB_2, on the other hand, superconducts at ~40 K at stoichiometry.

The light masses in MgB_2 enhance the phonon frequency ($\omega_{\rm ph} \propto M^{-1/2}$) that sets the temperature scale of T_c in BCS theory. Even considering this tendency, there must be some *specific feature(s)* that produces such a remarkable T_c, and moreover does so with no *d* electrons, nor even the benefit of a density of states (DOS) peak [10,11]. In this paper we identify these features: (1) hole doping of the covalent σ bands, achieved through the ionic, layered character of MgB_2, (2) 2D character of the σ band density of states, making small doping concentrations n_h give large effects $N(\varepsilon_F) \sim m^*/\pi\hbar^2$ independent of n_h, and (3) an ultrastrong deformation potential of the σ bands from the bond-stretching modes.

In this paper we exploit the similarities between graphite and MgB_2 to build a basic understanding of its electronic structure, then focus on the differences that are connected to strong EP coupling, and finally provide an estimate of T_c that indicates the picture we build can account for the observations. This picture further predicts that electron doping by ~0.2 carriers per cell will strongly affect T_c adversely, a result that has been reported by Slusky *et al.* [12]. Although Hirsch has also focused on the hole character of the σ bands [13], his emphasis is otherwise quite different from that described here.

Calculations of the electronic structure have been done using the linearized augmented plane wave (LAPW) method [14] that utilizes a fully general shape of density and potential, as implemented in the WIEN97 code [15]. Experimental lattice constants of $a = 3.083$ Å, $c = 3.521$ Å were used. LAPW sphere radii (R) of 2.00 a.u. and 1.65 a.u. were chosen for the Mg and B atoms, respectively, with cutoff $RK_{\rm max} = 8.0$, providing basis sets with more than 1350 functions per primitive cell. The generalized gradient approximation exchange-correlation function of Perdew *et al.* [16] was used in the present work.

 0031-9007/01/86(19)/4366(4)$15.00

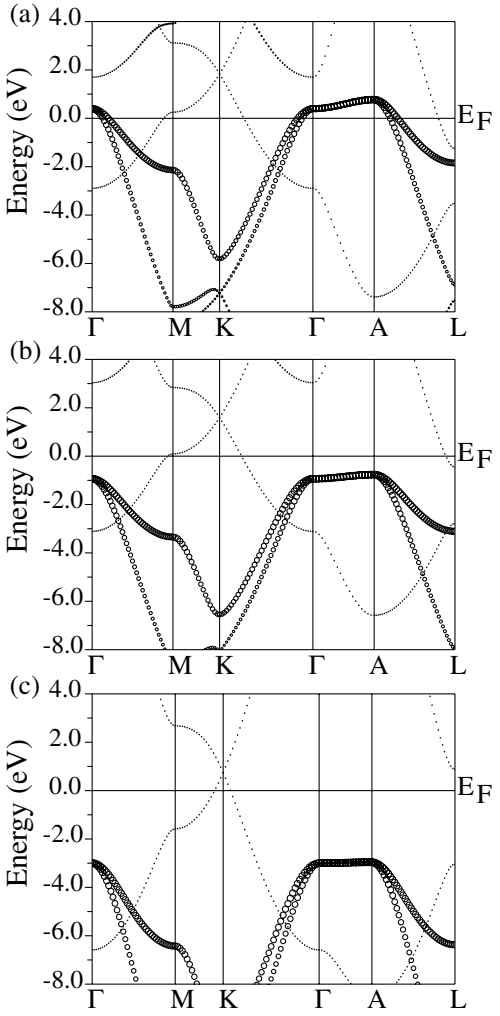

FIG. 1. Band structure along main hexagonal symmetry lines, for (top) MgB_2, (middle) $\square^{2+}B_2$, and (bottom) primitive graphite C_2. The planar σ states, highlighted with larger symbols, fall in energy in this progression, and only in MgB_2 are they partially unoccupied. The point $A = (0, 0, \pi/c)$ is perpendicular to the (k_x, k_y) plane.

The band structure of MgB_2 is shown in Fig. 1 (top panel) in comparison with that of primitive graphite (bottom panel) with a single layer per cell like the B_2 sublattice in MgB_2. For each two distinct sets of bands are identifiable: the highlighted sp^2 (σ) states and the p_z (π) states. The striking difference is in the position of the σ bands, which is evident in Fig. 1. Whereas the σ bonding states are completely filled in graphite and provide the strong covalent bonding, in MgB_2 they are unfilled and hence metallic, with a concentration of 0.067 holes/B atom in two fluted cylinders surrounding the Γ-A line of the Brillouin zone [10]. There are correspondingly more electron carriers in the π bands. This decrease in occupation on the strongly bonding σ bands partially accounts for the greatly increased planar lattice constant of MgB_2 (3.08 Å) compared to graphite (2.46 Å). Our results agree with previous conclusions that MgB_2 can be well characterized by the ionic form $Mg^{2+}(B_2)^{2-}$.

To identify the origin of the relative shift of the σ and π bands by $\sim$3.5 eV between graphite and MgB_2, we have considered a fictitious system $\square^{2+}B_2$ in which the Mg ion is removed but the two electrons it contributes are left behind (and compensated by a uniform background charge). The band structure, shown in the middle panel of Fig. 1, is very similar, except the energy shift of $\sim$1.5 eV downward with respect to MgB_2 completely fills the σ bands, as in graphite. This shift is the result of the lack of the attractive Mg^{2+} potential in MgB_2, which is felt more strongly by the π electrons than by the in-plane σ electrons: the attractive potential of Mg^{2+} between B_2 layers lowers the π bands, resulting in $\sigma \rightarrow \pi$ charge transfer that drives the hole doping of the σ bands. Belashchenko *et al.* [17] have also considered a sequence of materials to come to related conclusions about the band structure, but they did not use isoelectronic systems as has been done here.

The σ bands are strongly 2D (there is very little dispersion along Γ-A), but it will be important to establish the magnitude and effects of interplanar coupling. The light hole and heavy hole σ bands in MgB_2 can be modeled realistically in the region of interest (near and above ε_F) with dispersion of the form

$$\varepsilon_k = \varepsilon_0 - \frac{k_x^2 + k_y^2}{2m^*} - 2t_\perp \cos(k_z c), \qquad (1)$$

where the planar effective mass m^* is taken to be positive and $t_\perp = 92$ meV is the small dispersion perpendicular to the layers. The light and heavy hole masses are $m^*_{lh}/m = 0.20$, $m^*_{hh}/m = 0.53$, and the mean band edge is $\varepsilon_0 = 0.6$ eV. In general, the in-plane (v_{xy}) and perpendicular (v_z) Fermi velocities are expected to be anisotropic: $v_{xy} \sim k_F/m^*$, $v_z \sim 2ct_\perp$ where $t_\perp$ is small. Near the band edge ($k_F \leq 2m^* c t_\perp$) this anisotropy becomes small, and this is roughly the case in MgB_2. The π bands are also effectively isotropic [10,11].

Now we discuss why the quasi-2D character of the σ bands is an important feature of MgB_2 and its superconductivity. Neglecting the k_z dispersion, the 2D hole density of states is constant: $N_h^0(\varepsilon) = \frac{m^*_{lh}+m^*_{hh}}{\pi\hbar^2} = 0.25$ states/eV-cell, *independently of the fact that the hole doping level is small*. The k_z dispersion has only the small effect displayed in Fig. 2, where the discontinuity in the quasi-2D DOS is seen to be broadened by $\sim 2t_\perp$. For MgB_2 the σ band contribution to $N(\varepsilon_F)$ is reduced by about 10% by k_z dispersion.

If superconductivity is primarily due to the existence of holes in the σ band, and we provide evidence for such a picture below, then the DOS in Fig. 2 suggests that electron doping will decrease $N(\varepsilon_F)$. The decrease will be smooth to a doping level corresponding to an increase by 0.4 eV of the Fermi level. Then $N(\varepsilon_F)$ should drop precipitously with further doping. A rigid band estimate gives a value of

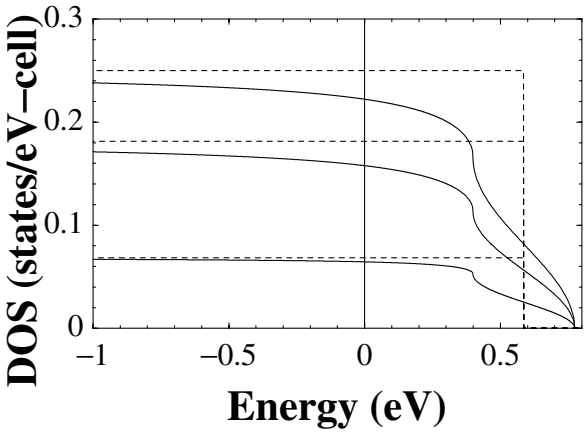

FIG. 2. Density of states (solid lines) of the light hole band, the heavy hole band, and the total, for the model of Eq. (1). Note that $N(\varepsilon)$ drops rapidly only 0.4 eV above ε_F. The dashed lines give the 2D ($t_\perp = 0$) analogs.

$n_{h,cr} = 0.08$ electrons necessary to fill the σ bands to the crossover region. Electrons must also be added to the π bands that lie in the same energy range, making the total doping level $n_{cr} \approx 0.25$ per cell.

Figure 2 therefore suggests a critical region of electron doping around 0.25 carriers per cell. Slusky *et al.* have reported [12] a study of such electron doping in the $Mg_{1-x}Al_xB_2$ system. T_c drops smoothly up to $x = 0.1$, beyond which point a two-phase mixture of B-rich and Al-rich phases occurs. At $x = 0.25$ and beyond, a single phase, nonsuperconducting system is restored, strongly supporting our picture that filling the σ bands will destroy superconductivity. Using the rigid band picture, filling them decreases T_c moderately initially, but as the σ bands become nearly filled, the coupling decreases abruptly and T_c vanishes, as observed. Although our results do not bear directly on the two-phase question, we note that this occurs just as the σ bands are filling. At this point $N(\varepsilon_F)$ is dropping, which normally favors stability. The observed instability suggests that a very small density of σ holes that are very strongly coupled to the lattice is what underlies the lattice instability.

Now we address the question of EP coupling strength λ. The calculated value of $N(\varepsilon_F) = 0.71$ states/eV-cell corresponds to a bare specific heat coefficient $\gamma_0 = 1.7$ mJ/mole-K^2. The available experimental estimate is [7] $\gamma_{\text{exp}} = (1 + \lambda)\gamma_0 = 3 \pm 1$ mJ/mole-K^2, giving $\lambda_{\text{exp}} \sim 0.75$. Kortus *et al.* [10] have used the rigid muffin tin approximation [18] to obtain an idea of the coupling strength. However, this approximation is not well justified in sp metals and neglects distinctions between bands of different character that we expect to be crucial for high T_c. If one assumes the wave vector dependence of coupling is not strong, there is another simple way to identify strong coupling using deformation potentials $\mathcal{D} \equiv \Delta\varepsilon_k/\Delta Q$ due to frozen-in phonon modes with mode amplitude Q [19]. The underlying concept is that a phonon that is strongly coupled to Fermi surface states will produce a large shift in ε_k for states near the Fermi level [19].

We have studied these deformation potentials for the $k = 0$ phonons B_{1g}, E_{2g}, A_{2u}, E_{1u}, whose energies, 86, 58, 48, 40 meV, respectively, have been calculated by Kortus *et al.* [10]. This mode (and others) destroys the symmetry of the crystal. The Brillouin zone remains unchanged, however, and we plot the bands along the same directions as in Fig. 1. This mode, as well as the B_{1g} mode, involves only out-of-phase motion of the two B atoms in the primitive cell, E_{2g} involving in-plane vibrations (bond stretching), B_{1g} having displacements perpendicular to the plane. In Fig. 3 the actual rms B displacement of $\Delta u_{\text{B}} = 0.057$ Å was used, to provide a clear picture of the very large effect of EP coupling strength.

The E_{2g} phonon strongly splits the σ band nearly uniformly all along the Γ-A line and near ε_F, with the "gap" opening $\Delta\varepsilon_{\text{gap}}/\Delta u_{\text{B}} = 26$ eV/Å $= 2\mathcal{D}_{E_{2g}}$; note that it will be the square of $\mathcal{D}$ that enters the expression (below) for λ. In stark contrast, the B_{1g}, A_{2u}, and E_{1u} modes produce no visible effect in the bands; we estimate that their deformation potentials are at least a factor of 25 smaller. Thus the only significant deformation potential is for the σ bands (π band shifts are always small), and only due to the E_{2g} mode. This one is extremely large, suggesting that nonlinear coupling may even be occurring. This strong coupling should be observable as a large E_{2g} linewidth, and the superconducting gap can be expected to be larger on the σ Fermi surface sheets than on the π sheets.

To estimate the coupling from this mode alone, we use Eq. (2.34) of Kahn and Allen [19] for the EP matrix element M in terms of $\mathcal{D}_{E_{2g}} = 13$ eV/Å, including only the two σ bands $N_\sigma = 0.11$ eV^{-1} per spin (from Fig. 2) and the two E_{2g} modes:

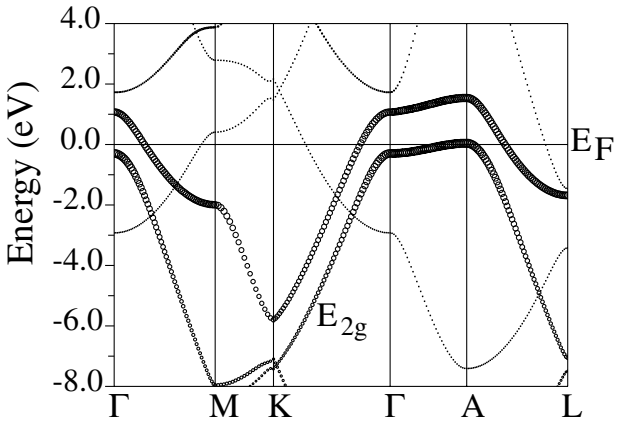

FIG. 3. Band structure with frozen-in E_{2g} mode, plotted along the same lines as in Fig. 1 to facilitate comparison. (Note that the point labeled K is no longer a symmetry point.) The E_{2g} phonon breaks the symmetry and splits the σ bands by 1.5 eV along Γ-A.

$$\lambda_{E_{2g}} = N_h(\varepsilon_F) \sum_{\nu=1,2} \left\langle \frac{|M^{\nu}_{k,k}|^2}{\omega_\nu} \right\rangle_{\varepsilon_F} \quad (2)$$

$$= 2N_h(\varepsilon_F) \left[\frac{\hbar}{2M_B\omega^2} \right] \left| \sum_{j=1,2} \hat{\boldsymbol{\epsilon}}_j \cdot \vec{\mathcal{D}}_j \right|^2 \approx 1.0 . \quad (3)$$

The sum on j runs over the two moving B atoms of the E_{2g} mode. Using this value of λ, the E_{2g} mode frequency, and the Allen-Dynes [20] or McMillan equation with Coulomb pseudopotential $\mu^* = 0.10-0.15$, the resulting range is $T_c = 32-46$ K. There is considerable uncertainty in this estimate, but it seems quite plausible that coupling of the σ band to the bond-stretching mode may provide most of the coupling to account for the observed value of T_c.

Now we summarize, beginning with the effects of low dimensionality mentioned in the introduction, as follows: (1) the B_2 layers provide a strong differentiation between B states (σ vs π) that results in the Mg^{2+} layer giving a 3.5 eV σ-π energy shift, driving self-doping of the σ bands; (2) because of their 2D dispersion, the contributions of the σ bands to $N(\varepsilon_F)$ is almost independent of the doping level; specifically, for low doping level $N_h(\varepsilon_F)$ is *not* small. Then, the strong covalent nature of the σ bands leads to an extremely large deformation potential for the bond-stretching modes. Judging from the very small deformation potentials of the other three Γ point modes, the bond-stretching modes dominate the coupling.

W. E. P. is grateful to P. C. Canfield for conversations and for early communication of manuscripts. This work was supported by Office of Naval Research Grant No. N00017-97-1-0956.

Note added.—Since this paper was submitted, two reports of EP coupling in MgB_2 that support our results [21,22] have come to our attention.

[1] J. R. Gavaler, Appl. Phys. Lett. **23**, 480 (1973).
[2] L. F. Mattheiss, E. M. Gyorgy, and D. W. Johnson, Jr., Phys. Rev. B **37**, 3745 (1988); R. J. Cava and B. Batlogg, Mater. Res. Bull. **14**, 49 (1989).
[3] T. T. M. Palstra *et al.,* Solid State Commun. **93**, 327 (1995).
[4] S. Yamanaka *et al.,* Adv. Mater. **9**, 771 (1996); S. Yamanaka, K. Hotehama, and H. Kawaji, Nature (London) **392**, 580 (1998); S. Shamoto *et al.,* Physica (Amsterdam) **306C**, 7 (1998).
[5] J. H. Schon, C. Kloc, and B. Batlogg, Nature (London) **408**, 549 (2000).
[6] J. Akimitsu, in Proceedings of the Symposium on Transition Metal Oxides, Sendai, 2001 (to be published); J. Nagamatsu *et al.,* Nature (London) **410**, 63 (2001).
[7] S. L. Bud'ko *et al.,* Phys. Rev. Lett. **86**, 1877 (2001).
[8] D. K. Finnemore *et al.,* cond-mat/0102114; G. Rubio-Bollinger *et al.,* cond-mat/0102242; B. Lorenz *et al.,* cond-mat/0102264; P. C. Canfield *et al.,* cond-mat/0102289; A. Sharoni *et al.,* cond-mat/0102325; H. Kotegawa *et al.,* cond-mat/0102334.
[9] I. T. Belash *et al.,* Solid State Commun. **64**, 1445 (1987).
[10] J. Kortus *et al.,* cond-mat/0101446.
[11] G. Satta *et al.,* cond-mat/0102358.
[12] J. S. Slusky *et al.,* cond-mat/0102262.
[13] J. E. Hirsch, cond-mat/0102115.
[14] D. J. Singh, *Planewaves, Pseudopotentials, and the LAPW Method* (Kluwer Academic, Boston, 1994).
[15] P. Blaha, K. Schwarz, and J. Luitz, WIEN97, Vienna University of Technology, 1997. Improved and updated version of the original copyrighted WIEN code, which was published by P. Blaha, K. Schwarz, P. Sorantin, and S. B. Trickey, Comput. Phys. Commun. **59**, 399 (1990).
[16] J. P. Perdew *et al.,* Phys. Rev. B **46**, 6671 (1992); J. P. Perdew, K. Burke, and M. Ernzerhof, Phys. Rev. Lett. **77**, 3865 (1996).
[17] K. D. Belashchenko, M. van Schilfgaarde, and V. P. Antropov, cond-mat/0102290.
[18] G. D. Gaspari and B. L. Gyorffy, Phys. Rev. Lett. **28**, 801 (1972).
[19] F. S. Khan and P. B. Allen, Phys. Rev. B **29**, 3341 (1984).
[20] P. B. Allen and R. C. Dynes, Phys. Rev. B **12**, 905 (1975).
[21] A. Y. Liu, J. Kortus, and I. I. Mazin (unpublished).
[22] Y. Kong *et al.,* cond-mat/0102499.